

A STUDY OF HEAT LOSS THROUGH BASEMENT FLOORS

W.R. Richmond R.W. Besant
 ASHRAE Member

ABSTRACT

In this paper, heat losses from basement floors are investigated by measuring the temperature distributions and heat rates for a period of one year across the basement floor insulation in two houses on the Canadian prairies. These experimental results are compared with two existing design models as well as a finite element model. The existing design models for basement floor heat losses with basement floor insulation appear to give good results for total heat loss over the year in spite of the fact that transient effects are not well modelled and internal radiation heat transfer is neglected. A parametric study of heat losses using a steady-state finite element model shows the importance of various factors including subfloor insulation, insulation bridges, interior radiation, soil conduction, etc. The transient finite element model shows good agreement with measured data on a daily, monthly, and yearly basis.

INTRODUCTION

With the advent of energy conservation homes (homes with annual heating requirements, normalized with respect to floor area and seasonal degree days, of less than 1.6 Btu/ft²DD(F) (33 KJ/m²DD(°C)) it has become apparent that existing methods of predicting heat loss from basements such as those given in the 1985 ASHRAE Fundamentals are inadequate. The methods presented do not deal with various methods of insulating basements. Accuracy of the methods, while adequate for conventional housing of the 1970s, are inadequate for the energy conservation home. As a result, various researchers within the past few years have given the basement heat loss problem a great deal of attention. Their interest has also been prompted by the need for methods that can be programmed easily for a personal computer for use as a design tool.

The problem of predicting heat losses from below grade surfaces in basements is a difficult one. In comparison, the heat loss from the upper floors of a residential dwelling are easily predicted. The above grade surfaces have well-defined boundaries, more easily determined boundary conditions, and high thermal resistances. Below grade surfaces, on the other hand, have boundaries which lose heat to the surrounding soil. In uninsulated basements the thermal resistance of the walls and floor are of the same order as that of the surrounding soil. Soil thermal conductivity is dependent on a number of factors, such as the mineral and organic material content, density, water content, and temperature. Estimating the soil thermal conductivity from soil content and density by analytical methods can at best be described, in the absence of a large number of measurement and chemical analyses, as more of an art than a science. Furthermore, the temperature distribution within the surrounding soil is also dependent on a number of factors such as air temperature, solar radiation, vegetation and snow ground cover, and wind velocities. Finally, soil temperature distribution and heat transfer may also be affected by the movement of ground water through the soil and any phase change.

W.R. Richmond, Graduate Student, and R.W. Besant, Professor and Head, Department of Mechanical Engineering, University of Saskatchewan

Interest in basement heat loss is not only concerned with the problem of calculating the magnitude of heat loss but also with how it affects the comfort of the basement area. In a study by Besant et al. (1982) of 14 energy conservation homes in Saskatoon in which the basement walls were heavily insulated while the floors remained uninsulated, it was found that up to 50% of the total heat loss from the homes was lost through the uninsulated basement floor. More important, perhaps, was the finding that the basements of several of these homes were unsuitable as living space because of low floor temperatures. Heating requirements for these basements extended over the full year whereas the upper living areas required somewhat continuous heating over five to six months of the year and intermittently over another two or three months. In the conventional, less energy efficient home the longer periods of time during which heat is required during the heating season and the larger natural heat gains during summer are sufficient to meet basement heating requirements.

Because of the research by Besant et al. (1982) it was decided to conduct a study of basement floor heat loss in residential dwellings. Two homes were monitored in the period between December 1982 and June 1984 (Richmond et al. 1984) for air, floor, and subsoil temperatures as well as electrical, gas, and water consumption. In addition, it was decided to compare the heat losses measured at these two homes to the literature for predicting basement floor heat loss. A finite element study of one of the homes would also be conducted to experiment with some of the parameters involved in the basement heat loss problem. The purpose of this paper is to present some of the results of those investigations.

DESCRIPTION OF EXPERIMENTAL INVESTIGATION

The first home, herein referred to as House 1, was a 1200 ft² (110 m²) three-bedroom bungalow with a 1170 ft² (108 m²) full concrete basement built in 1968 to conventional standards of that time with no basement insulation. This house was retrofitted by the Division of Building Research, National Research Council of Canada, in the late summer of 1982. The exterior of the house above ground was wrapped with a vapour barrier and R40 (RSI 7.0 m² K/W) insulation and enclosed with plywood. The interior of the basement walls received a vapour barrier and the same level of insulation. The concrete basement floor was insulated in December 1983 with the addition of R15 (RSI 2.6) extruded polystyrene insulation on top of the existing floor and covered with 5/8 in (16 mm) plywood. Above grade, double-glazed windows received an additional pane of glass. The house was electrically heated with two 1500-watt heaters on the main floor and one 2000-watt heater in the basement. The house was monitored through the use of a remote data acquisition system from late December 1982 through June 1984 during which time the house was unoccupied. The basement floor plan with the floor temperature measurement sites is illustrated in Figure 1.

The second home, herein referred to as House 2, was privately constructed during the winter of 1982-1983 to low energy housing standards. The two storey home consists of a floor area of approximately 980 ft² (91 m²) on the second storey, 940 ft² (87 m²) on the main floor, and 990 ft² (92 m²) in the basement. The concrete walls in the full basement were insulated on the inside with R24 (RSI 4.2) insulation, and the concrete basement floor was laid on top of R10 (RSI 1.8) extruded polystyrene insulation. Heating was provided by a conventional gas hot air furnace. The house was occupied in April 1983 and monitoring effectively covered the period from late July 1983 to June 1984. The basement floor plan for the house with the sites at which the floor temperatures were measured is illustrated in Figure 2.

The heat flux through the basement floors of both homes was calculated by measuring the temperatures above and below the extruded polystyrene insulation. Knowing the temperature difference across the insulation and the R-value of the insulation, the heat flux through the insulation could be calculated. Cross sections of the insulation arrangements for the two houses are illustrated in Figure 3.

PARAMETRIC STEADY-STATE FINITE ELEMENT STUDIES

To determine the effect of various parameters, such as soil thermal conductivity, external and internal heat transfer coefficients, internal and external temperatures, and floor insulation conductivities, a steady-state finite element model was used. A reference or base case, about

which the parameters were varied, was selected so as to determine the effects that the various changes and ranges of each parameter would have. A general purpose, commercially available finite element package was used for modelling purposes.

The basic model, shown in Figure 4, patterned on the basement of House 2, consisted of 319 nodes and 468 elements. One unique feature of the model was the inclusion of 155 two-node radiation elements to simulate radiation exchange between the surfaces in the basement. The remainder of the elements were four and eight-node isoparametric elements with a few triangular elements. The model was composed of four materials -- concrete, extruded polystyrene insulation, glass fibre insulation, and soil. Because of the special interest in basement floor heat loss, the thermal conductivity of the polystyrene insulation was considered to be temperature dependent. However, over the range of temperatures encountered, temperature variations make little difference in the R-value of the insulation. The thermal conductivity of the glass fibre insulation was modified to take into account the wood studs in the wall cavity.

The reference base case to which the comparisons were made was based on average conditions for the month of January 1984. For this base case heat transfer coefficients along the floor and walls of the model were selected to be $0.26 \text{ Btu/h}\cdot\text{ft}^2\cdot\text{F}$ ($1.5 \text{ W/m}^2\cdot\text{K}$), $0.083 \text{ Btu/h}\cdot\text{ft}^2\cdot\text{F}$ ($0.47 \text{ W/m}^2\cdot\text{K}$) along the exterior above grade portion of the basement wall, and $0.58 \text{ Btu/h}\cdot\text{ft}^2\cdot\text{F}$ ($3.3 \text{ W/m}^2\cdot\text{K}$) along the ground surface and included the effect of snow cover. The air temperature along the surface of the floor was set at 65.1 F (18.4°C) while the ceiling temperature was 68.5 F (20.3°C). The deep ground temperature for the model was 44.8 F (7.1°C) as determined by the equation of Kusuda and Achenbach (1965) and verified in field measurements. Outdoor air temperature was 10.2 F (-12.1°C). Emissivity of the wall, floor, and ceiling surfaces were assumed to be 0.9. Shape factors between the floor and ceiling, floor and wall, and wall and ceiling were calculated using Hottel's method (Sparrow and Cess 1978) for two-dimensional radiation exchange between surfaces.

Using the boundary conditions outlined above it was found that radiation was the major mode of heat transfer between the basement ceiling and the basement floor surface. In the base case the floor experiences a heat loss of $35.4 \text{ Btu/h}\cdot\text{ft}$ (34.0 W/m). The floor gains $41.2 \text{ Btu/h}\cdot\text{ft}$ (39.6 W/m) by radiation while losing $5.8 \text{ Btu/h}\cdot\text{ft}$ (5.6 W/m) by convection to the air above the floor. For typical cases with this model, radiation plays a major role in the heat transfer exchange mechanisms occurring in the basement. A literature search by the authors has not uncovered any other such finding. The average temperatures used for the ceiling and the air temperature near the floor represent the time average values calculated from measured temperatures. Although this parametric model study is steady-state, the same heat transfer mechanisms occur in the transient finite element model discussed later in this paper. To further investigate the role of radiative heat transfer in the model, two test cases were run where radiative heat transfer was eliminated. In the first instance, nothing else was changed and in the second instance the heat transfer coefficients along the wall and floor were changed to include the effect of radiative heat transfer. As a result, in the first instance there was a decrease of 19% for the floor heat loss from the base case, while in the second there was only a 11.7% decrease. While adjustment of the heat transfer coefficients provides a means of compensating for the lack of radiative heat transfer, it nonetheless fails to account for the nature of the heat transfer processes occurring and may result in errors of the order of 10%. By using only convection and conduction in the model the air must lose energy to the floor, that is, the floor temperature must be lower than the air temperature. In this case, while floor surface temperatures drop only an average of 2 F (1 K) this drop could be significant in terms of occupancy comfort in the basement. As such, neglecting radiative heat transfer could lead to serious errors in the determination of occupancy comfort.

The air temperature above the floor, the ceiling temperature, and the convection coefficients used along the wall and floor were varied to determine the effect of each. Increasing the ceiling temperature by 3.1 F (1.7 K) caused an increase in the floor heat loss of 8.3%, while increasing the air temperature above the floor by 3.4 F (1.9 K) only increased the floor heat loss by 3.5%. As well as incurring a greater heat loss, the increase in ceiling temperature resulted in a significant increase in the surface temperature of the concrete of $2\text{--}3 \text{ F}$ ($1\text{--}2 \text{ K}$) while the increase in the air temperature above the floor resulted in only a very slight increase in floor temperature over the base case. These results indicate that radiant heating in a basement may be more effective in terms of occupant

* Heat losses are given per unit length since the model used was two-dimensional.

comfort than forced air heating. Variation of the heat transfer coefficients along the floor and wall in the range of 0.2-0.7 Btu/h·ft²·F (1-4 W/m²·K) result in an increase over that range of 1.8%. These results would tend to confirm that radiation plays a major role in the heat losses incurred in the basement.

The deep ground temperature was another parameter that was examined. A 1.8 F (1.0 K) temperature change in the soil plane 16.8 ft (5.1 m) below the ground surface from the base case resulted in a change in the floor heat loss of 5.6%. At that depth, the amplitude of the soil temperature range over the year is expected to be, on average, 4.9 F (2.7 K).

Other climatic parameters that would influence the basement are outdoor temperature, solar radiation, and ground cover. Decreasing the ambient outdoor temperature by 14.2 F (7.9 K) increased the floor heat loss by 6.9%. The base case model did not take into consideration the solar insolation received during the month of January. Because of the high reflectivity of the snow, and with the assumption of snow cover, the effect of solar insolation would be negligible. However, during the summer it could be significant. To observe the effect of solar insolation the average conditions for the month of August were used in the model as the base case. One case was run with the average outdoor air temperature and the other with the average sol-air temperature for the month. Overall there was a 16% decrease in total basement heat loss including the walls from the first to the second case with a decrease of 5% in the floor heat loss. In the base case, the exterior heat transfer coefficient was modified to include the snow cover present during January. By changing the exterior heat transfer coefficient so as not to include the snow cover, there was a 6.8% increase in the overall heat loss with 11.4% resulting from the walls and 2.4% from the floor. In these cases, in which the ground surface layer parameters were varied, the basement walls were more sensitive to the changes than the basement floor, as might be expected. In the case where the deep soil temperature was varied, the basement floor was found to be more sensitive to changes than were the walls.

The effect of various insulation strategies was also investigated. In changing the R-value of the floor insulation to the equivalent resistance of the soil beneath it, the floor heat loss increased by 61% while the wall heat loss decreased by 4%. Doubling the R-value of the floor insulation produced a decrease of 22% in the floor heat loss while increasing the wall heat loss by 1%. Halving the R-value of the floor insulation increased the floor heat loss by 21% and decreased the wall heat loss by 1%. Referring to Table 1, it can be seen that a large discrepancy of 40-60% exists between the actual heat loss through the perimeter of the basement floor and that conducted vertically through the insulation. This would indicate that heat is being lost horizontally as well as vertically through the basement floor. To investigate this further, an insulated thermal barrier was introduced into the model through the substitution of a piece of insulation for the concrete at the intersection of the footing and the concrete floor. This resulted in a 10% decrease in the floor heat loss and a 1% increase in the wall heat loss. It also resulted in an increase in the floor temperatures near the wall, which would thereby improve the thermal comfort of the basement floor. Lastly, outside perimeter insulation was introduced in the model protruding 2 ft (0.6 m) outside the basement wall just above the foundation footing. The model showed a negligible improvement in the heat loss from the basement in this case.

The last parameter that was varied was the soil thermal conductivity. In the test cases examined the soil thermal conductivity, which was assumed to be homogeneous throughout the model, was varied from 5.2-15.6 Btu in/h·ft²·F (0.75-2.25 W/m K). It was found that over the range of thermal conductivities tested, the changes in heat losses were nearly linearly related to the changes in soil thermal conductivity. Increasing the thermal conductivity of the soil to 15.6 Btu·in/h·ft²·F (2.25 W/m·K) increased the total basement heat loss by 22% with the basement walls experiencing a 9% increase and the floor a 33% increase. The basement wall is less sensitive to changes in the soil thermal conductivity than the basement floor.

MODELLING BASEMENT HEAT LOSS

Three methods of modelling the basement floor heat loss were found to be practical for the houses studied and for the severe winter climate experienced on the Canadian prairies. The first two are previously published methods by Mitalas (1982, 1983) and by Yard et al. (1984). The third is a transient finite element model based on the same model geometry as that for the steady-state model previously discussed.

Transient Finite Element Model

Because of the time required to assemble the transient finite element model and the transient physical effects present in House 1, only House 2 was modelled. The model geometry and material properties were identical to that of the steady-state model used in the parameter study with the exception that the thermal conductivity of the extruded polystyrene insulation was made temperature invariant. Studies done on the steady-state model indicated that over the temperature ranges encountered by the insulation, the error introduced would be less than 0.5%. Using a constant thermal conductivity for the floor insulation resulted in a large saving in the computer time required to run the model. In modelling the transient behavior of the basement average basement temperatures, the ambient or sol-air temperature, the deep soil temperature, and the exterior heat transfer coefficient for each month were assumed to exist at the middle of the month. These boundary conditions were then linearly varied between months. To start the model the initial conditions input were the steady-state results for the month of June. Two complete "years" were run. After the second year the final conditions were identical to the initial conditions.

Because the model was two-dimensional, the heat losses generated by the model had to be translated to three dimensions. This was accomplished by multiplying the heat loss for each section of the basement (i.e. wall above grade, floor perimeter, etc.) by the area of the section divided by the two-dimensional "length" of the model section.

The floor temperature profiles of the basement floor and insulation are presented in Figure 5, and the heat loss profiles for the floor are presented in Figure 6 for the date January 6, 1984. Data illustrated were obtained from the temperatures and heat losses at each node of the model. Spline curves have been drawn through the points. From these figures it can be seen that both the heat loss and temperature are a function of the distance away from the centre of the model. The temperatures and heat flux remain relatively uniform along the floor until reaching the perimeter zone of the basement. Once the perimeter is reached, the temperatures begin to drop quite dramatically, especially near the basement wall. At the soil-insulation boundary beneath the concrete floor, the temperature profile is much more moderate and begins a gradual downward trend approximately 7 ft (2 m) from the centre of the floor. Similarly, the heat transfer rates increase rapidly in the perimeter area. The conductive heat loss curve (representing the heat actually lost through the basement floor) may be thought of as the radiative heat gain curve (from radiant energy exchange with the ceiling and the wall) minus the convective heat loss curve (heat loss by the floor to the air above the floor). As was previously demonstrated in the steady-state model, radiation plays a very major role in the heat loss process occurring.

Mitalas' Model

Modelling of both houses using Mitalas' (1983) model was undertaken. Use of Mitalas' model is awkward in that while Mitalas represents a number of insulation configurations for use by the designer, their range of parameters is limited. They are limited in that for one large group of cases the assumption is made that the insulation levels are the same for both the floor and the walls, while in the cases where Mitalas has presented the coefficients for differing R-values for the floor and walls the selection is quite narrow. Therefore the designer must either discard the method because of its limitations or apply the method in a manner for which it was not designed. In this instance, the authors chose the latter.

Yard et al. Model

Use of the Yard et al. model (1984) was possible only with House 2. Yard's model is not capable of modelling basements with very high insulation levels. Modelling of House 1 with the method was attempted, but the wall heat conductance coefficient generated was negative. Therefore the method was not used for House 1.

COMPARISON OF METHODS

House 1

Figure 7 illustrates the results of Mitalas' model and the measured data taken at the house from late December 1983 to June 1984. The measured data were obtained from nine sites where the temperatures above and below the insulation were measured. Three sites were located in the perimeter zone (sites A, J, and E in Figure 1), and the rest (sites M, N, S, O, Q, P) were located in the interior zone of the floor. To obtain the heat flux at each site, the temperature difference across the insulation was divided by the R-value of the insulation. The interior heat loss was the result of taking the average of the heat fluxes at the six sites and multiplying by the area of the interior zone. At the perimeter, the heat loss was the result of taking the sum of the heat flux at sites A and E and twice the heat flux at site J, dividing by 4 and then multiplying by the perimeter area. The measured data presented represent the instantaneous values taken at 15-minute intervals over the period of time shown. Comparison of Mitalas' values to the measured data yields little agreement between the two sets of curves. However, the measured data, while representing what actually occurred at the house, does not represent the conditions modelled by Mitalas. The placement of insulation on the basement floor introduces a large disturbance in the seasonal variation in basement floor heat loss over a typical year. In this case, heat loss would likely have been less during the first few months of measured data presented in Figure 7 than if the insulation had been on for a least a year or two. This would be because of the high soil temperatures beneath the basement floor just before it was insulated. After insulation was placed on the concrete floor, the large thermal mass of the soil would necessitate a time period for the soil temperatures beneath the basement floor to reach some sort of a quasi-steady-state value. This is seen in Figure 8, which represents the soil temperatures beneath Site N in Figure 1. It appears that by the end of June, the temperatures are beginning to reach a quasi-equilibrium condition. However, comparison between Mitalas' model and the measured data, while improved, still shows substantial differences. During the period from January 1984 to June 1984, the measured perimeter heat loss was 1.52 million Btu (1.60 GJ), and the measured interior heat loss was 2.22 million Btu (2.35 GJ). Mitalas' model predicted a perimeter heat loss of 3.36 million Btu (3.55 GJ) and a interior heat loss of 3.36 million Btu (3.49 GJ).

House 2

Figure 9 represents measured data taken over a period from July 1983 to June 1984 and the predicted heat loss generated by the transient finite element model over the same time period.

The measured data presented have been condensed to monthly average values with a smooth curve drawn between the points. The measured data are taken from hourly temperatures at seven sites on the floor, two in the perimeter zone (Sites A and G in Figure 2) and the rest (Sites B-F) in the interior zone. Heat fluxes for each site were calculated in the same manner as for House 1. Because of the two-dimensional nature of the heat loss in the perimeter zone (as shown by the finite element model), the averaged heat flux from the two sites was multiplied by a time variant factor calculated from the transient finite element model to obtain the heat loss from the perimeter. The interior heat loss was obtained by multiplying the average of the five heat fluxes in the interior by the interior floor area.

The transient finite element model data presented in Figure 9 are more continuous, and the data points have not been defined on the graph. As can be seen, there appears to be very good agreement between the measured data and the transient model. While there is some disagreement in the magnitudes of the heat losses, there is good agreement in the shape and trends of the curves.

Figure 10 represents the total predicted basement floor heat loss generated by Mitalas' model, the Yard et al. model, and the transient finite element model. Mitalas' monthly averaged totals are shown as symbols on the graph with a smooth curve connecting them. Yard's curve is the result of daily totals calculated for the floor. The transient finite element curve seen is the same as in Figure 9. Mitalas' calculations are based on an average variation of the ground surface temperature, while Yard's method is based on the ambient air temperature. This may be seen in the smooth curves generated by both of those models. The finite element model in contrast is much less smooth and, as is seen in Figure 9, follows the measured data much more closely. The curve generated by Yard's model has a much larger amplitude than Mitalas', the finite element model, or the measured data. The results from

Mitalas' model have the smallest amplitude.

Table 2 outlines the total yearly heat loss for the measured data and for the models. In the yearly total, Mitalas' model was the closest to the measured data with a -3.1% difference, followed by the transient finite element model with 7.3% difference, and by Yard's model with a -16.5% difference. Table 2 also makes a comparison between the total required for a seven-month heating season for the measured data and the models. Perhaps this is a more realistic comparison in that this represents the heating load the homeowner must pay for. During the other months of the year, heating would not be required for the upper floors of the house, and therefore the basement would not be heated unless auxiliary heating is supplied to make the basement area comfortable as a living space. In this comparison there is a 4.4% difference between the measured data and Mitalas' model, -5.1% with Yard's model, and 8.7% with the transient finite element model.

CONCLUSION

Two-dimensional finite element studies conducted demonstrate the importance of radiation in the heat transfer processes occurring in a basement. Studies also demonstrate that the elimination of thermal contact between the basement floor slab and the basement wall footing reduces basement floor heat loss while increasing the floor temperature.

Use of the Yard et al. (1984) model for high levels of insulation used on basement walls for houses in the Canadian prairies was not possible. The model, when compared to the measured results from a house with lower insulation levels, had a much higher amplitude of heat loss over the year and disagreed with the trends and amount of heat loss exhibited in the measured data. Compared on a yearly basis with the measured data, the error in the total yearly heat loss was greater than any of the other models.

Mitalas' (1983) model, as well, was incapable of modelling the transient phenomenon exhibited in the measured data. However, when yearly totals were compared over both the year and the heating season, agreement with the measured data was within plus or minus five percent.

The transient finite element model was the most promising of the three models tested. Its predictions were seen to closely model what was occurring in the physical data on a monthly basis. Energy totals for the year and heating season were within 9% of the measured data, which is estimated to be within the range of experimental uncertainty.

REFERENCES

- ASHRAE. 1981. ASHRAE Handbook--1981 Fundamentals, pp. 25.6-25.8. Atlanta: American Society of Heating, Refrigerating, and Air-Conditioning Engineers, Inc.
- ASHRAE. 1977. ASHRAE Handbook--1977 Fundamentals, pp. 24.3-24.5. Atlanta: American Society of Heating, Refrigerating, and Air-Conditioning Engineers, Inc.
- Besant, R.W.; Hamlin, T.; and Richmond, W. 1982. "Dynamics of heat losses from uninsulated basement floors in houses." Proceedings of the ASHRAE/DOE Conference Thermal Performance of the Exterior Envelopes of Buildings II. Atlanta: American Society of Heating, Refrigerating, and Air-Conditioning Engineers, Inc.
- Kusuda, T; and Achenbach, P.R. 1965. "Earth temperature and thermal diffusivity at selected stations in the United States." ASHRAE Transactions, Vol. 71, Part 1, pp. 61-75.
- Mitalas, G.P. 1983. "Calculation of Basement Heat Loss." ASHRAE Transactions, Vol. 89, Part 1B, pp. 420-437.
- Richmond, W.R.; Besant, R.W.; Watson, L.G. 1984. "Temperatures and Heat Losses in Basement Floors With and Without Subfloor Insulation." Proceedings of the 10th Annual National Conference of the Solar Energy Society of Canada. Winnipeg: Solar Energy Society of Canada Inc.

Sparrow, E.M.; and Cess, R.D. 1978. Radiation Heat Transfer. Washington: Hemisphere Publishing Corporation.

Yard, D.C.; Morton-Gibson, M.; and Mitchell, J.W. 1984. "Simplified dimensionless relations for heat loss from basements." ASHRAE Transactions, Vol. 90, Part 1, pp. 633-643.

BIBLIOGRAPHY

MacDonald, G.R.; Claridge, D.E.; and Oatman, P.A. 1985. "A comparison of seven basement heat loss calculation methods suitable for variable-base degree-day calculations." ASHRAE Transactions, Vol. 91, Part 1.

Swinton, M.C.; Platts, R.E. 1981. "Engineering method for estimating annual basement heat loss and insulation performance." ASHRAE Transactions, Vol. 87, Part 2, pp. 343-359.

Kuehn, T.H. 1982. "Temperature and Heat Flow Measurements From an Insulated Concrete Bermed Wall and Adjacent Floor." Journal of Solar Energy Engineering, Transactions of the ASME, Vol. 104, Feb. 1982, pp. 16-22.

Kusuda, T.; and Bean, J.W. 1984. "Simplified methods for determining seasonal heat loss from uninsulated slab-on-grade floors." ASHRAE Transactions, Vol 90, Part 1B, pp. 611-632.

ACKNOWLEDGMENTS

The cooperation and assistance of the Division of Building Research, National Research Council of Canada, Saskatoon, Saskatchewan in the research which was conducted is gratefully acknowledged.

TABLE 1
Results of Steady State Finite Element Simulations

Units of Heat Loss are Btu/h. ft
(Numbers in brackets are in units W/m)

Run Description	Basement Wall Losses				Basement Floor Losses			Total Basement	Vertical Loss Through Insulation		
	Above Grade	0-0.6m Below Grade	0.6m to Floor	Total Wall	1 m Perimeter	Interior Zone	Total	Loss	1 m Perimeter	Interior Zone	Total
Base Case	7.0 (6.7)	6.9 (6.6)	19.6 (18.8)	33.4 (32.2)	13.7 (13.2)	21.7 (20.9)	35.4 (34.0)	68.8 (66.2)	6.0 (5.8)	21.4 (20.6)	27.4 (26.3)
Radiation Eliminated	6.5 (6.3)	6.3 (6.0)	15.4 (14.8)	28.2 (27.1)	10.3 (10.0)	18.4 (17.6)	28.7 (27.6)	56.9 (54.7)	4.5 (4.4)	17.7 (17.0)	22.2 (21.4)
Radiation Eliminated $h_{\text{floor}} = 6.1 \text{ W/m}^2\text{-}^\circ\text{C}$, $h_{\text{wall}} = 8.3 \text{ W/m}^2\text{-}^\circ\text{C}$	7.7 (7.4)	6.8 (6.5)	21.6 (20.8)	36.1 (34.7)	11.9 (11.4)	19.4 (18.6)	31.3 (30.0)	67.4 (64.8)	5.7 (5.5)	19.2 (18.5)	25.0 (24.0)
No Floor Insulation	6.9 (6.7)	6.8 (6.5)	18.3 (17.6)	32.0 (30.8)	20.7 (19.9)	36.2 (34.8)	56.9 (54.7)	88.9 (85.5)	n/a	n/a	n/a
R Value Insulation 1/2 x Base Case	7.0 (6.7)	6.8 (6.6)	19.2 (18.4)	33.0 (31.7)	15.5 (14.9)	27.5 (26.4)	43.0 (41.3)	75.9 (73.0)	8.7 (8.4)	27.1 (26.1)	35.8 (34.4)
R Value Insulation 2 x Base Case	7.0 (6.8)	6.9 (6.6)	20.0 (19.2)	33.9 (32.6)	12.2 (11.8)	14.9 (14.4)	27.5 (26.4)	61.4 (59.0)	3.8 (3.6)	15.0 (14.4)	18.7 (18.0)
Thermal Barrier Between Floor and Footing	7.0 (6.8)	6.9 (6.7)	19.8 (19.0)	33.7 (32.4)	9.7 (9.4)	22.0 (21.2)	31.7 (30.5)	65.5 (63.0)	6.6 (6.3)	21.8 (20.9)	28.3 (27.2)
Insulation Around Outside Perimeter Of Footing	7.0 (6.7)	6.9 (6.6)	19.6 (18.8)	33.5 (32.2)	13.6 (13.1)	21.6 (20.8)	35.2 (33.9)	68.7 (66.1)	5.9 (5.7)	21.4 (20.6)	27.3 (26.2)
Soil Thermal Conductivity Equal to 2.25 W/m.K	7.1 (6.9)	7.1 (6.8)	22.3 (21.4)	36.5 (35.1)	16.9 (16.3)	30.2 (29.0)	47.1 (45.3)	83.7 (80.4)	7.8 (7.5)	29.9 (28.7)	37.6 (37.4)

TABLE 2
 Comparison of Measured and Predicted
 Basement Floor Heat Losses for House 2

Units of heat loss are 10^6 Btu
 (Numbers in brackets are in units GJ)

Description	Total Perimeter Loss For The Year	Total Interior Loss For The Year	Total Loss For Year	Total Loss Over Heating Season (Oct-Apr)
Measured	6.61 (6.97)	3.79 (4.00)	10.40 (10.97)	5.78 (6.10)
Transient Finite Element Model	5.67 (5.98)	5.49 (5.79)	11.16 (11.77)	6.28 (6.63)
Mitalas' Model	6.30 (6.65)	3.77 (3.94)	10.08 (10.63)	6.04 (6.37)
Yard, et al. Model	n/a	n/a	8.68 (9.16)	5.49 (5.79)

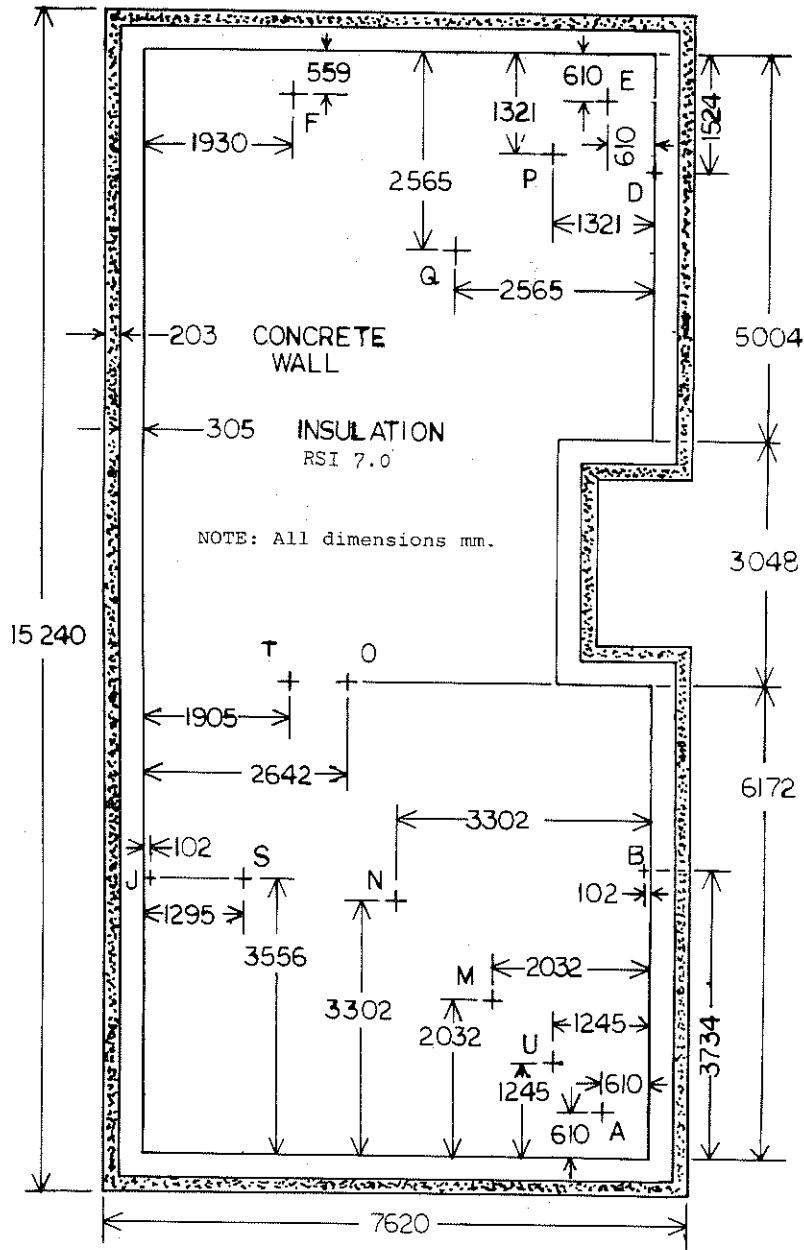


Figure 1. Basement floor plan of House 1

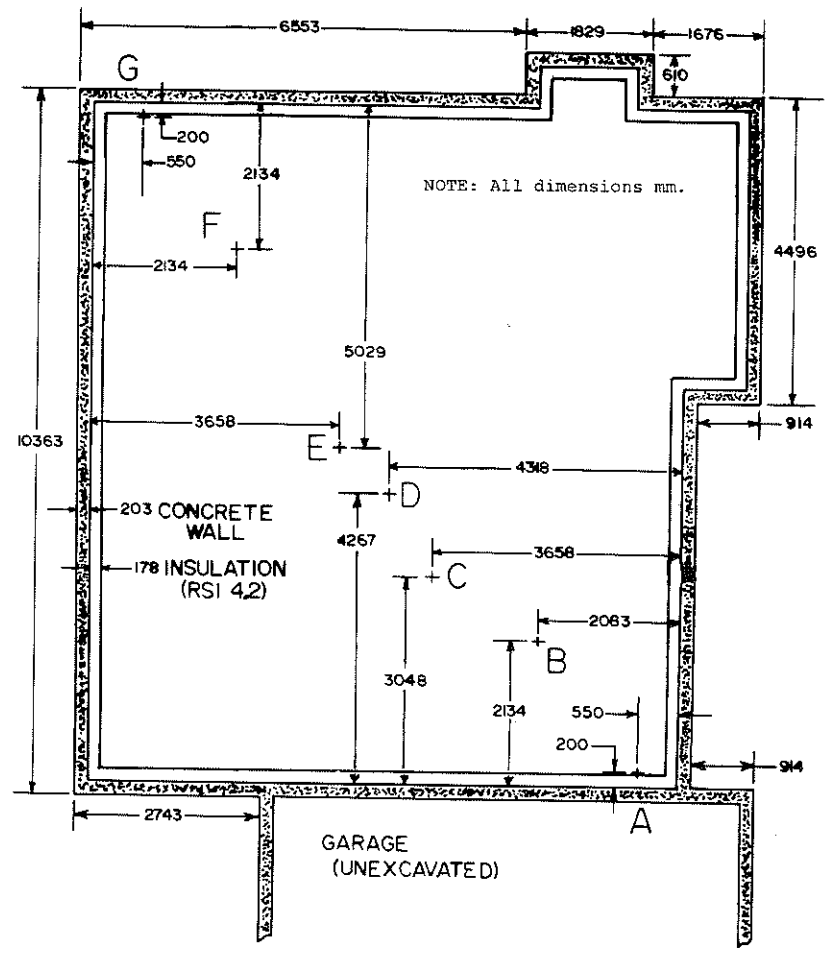
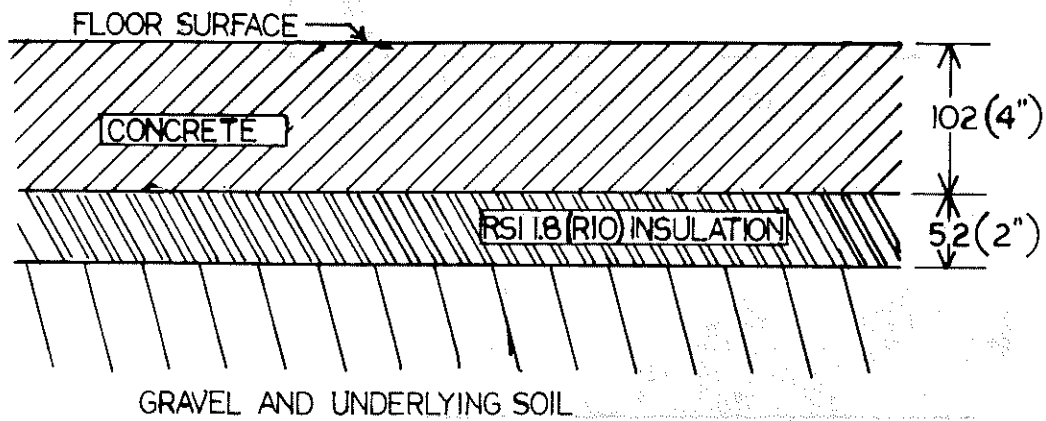
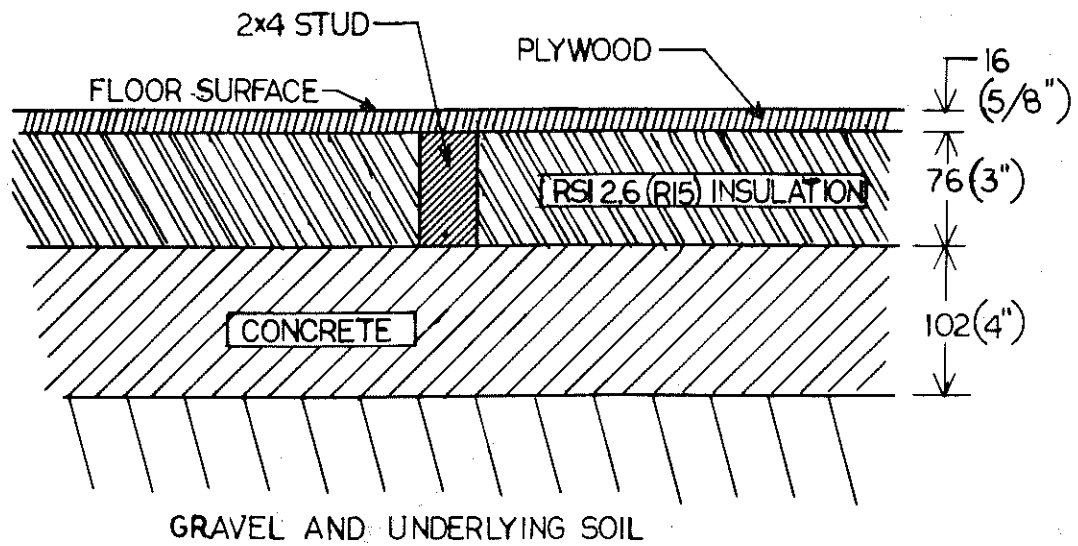


Figure 2. Basement floor plan of House 2



NOTE: All dimensions are in mm unless otherwise indicated.

Figure 3. Basement floor plan insulation arrangements for House 1 (top) and House 2 (bottom)

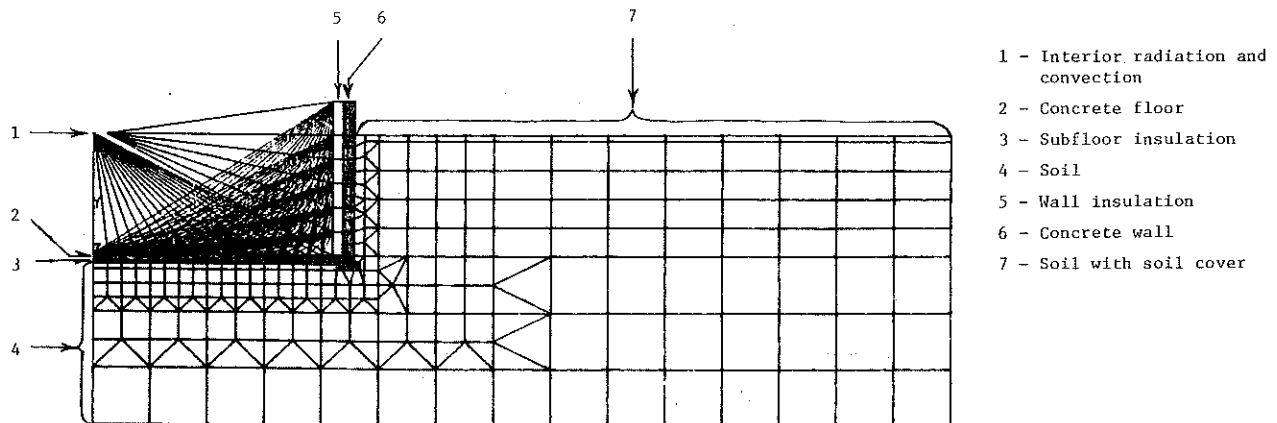


Figure 4. Two-dimensional finite element model

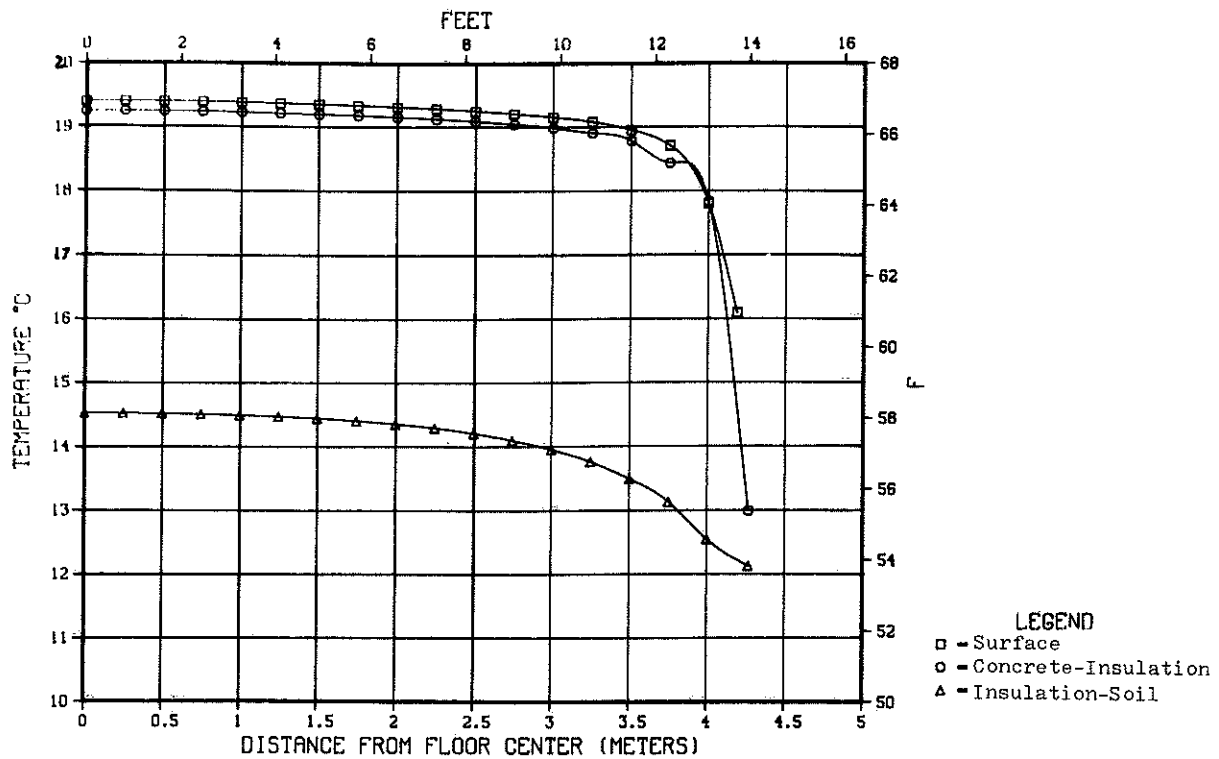


Figure 5. Temperature profiles for House 2 at and below basement floor surface. Transient finite element model simulation, January 6, 1984

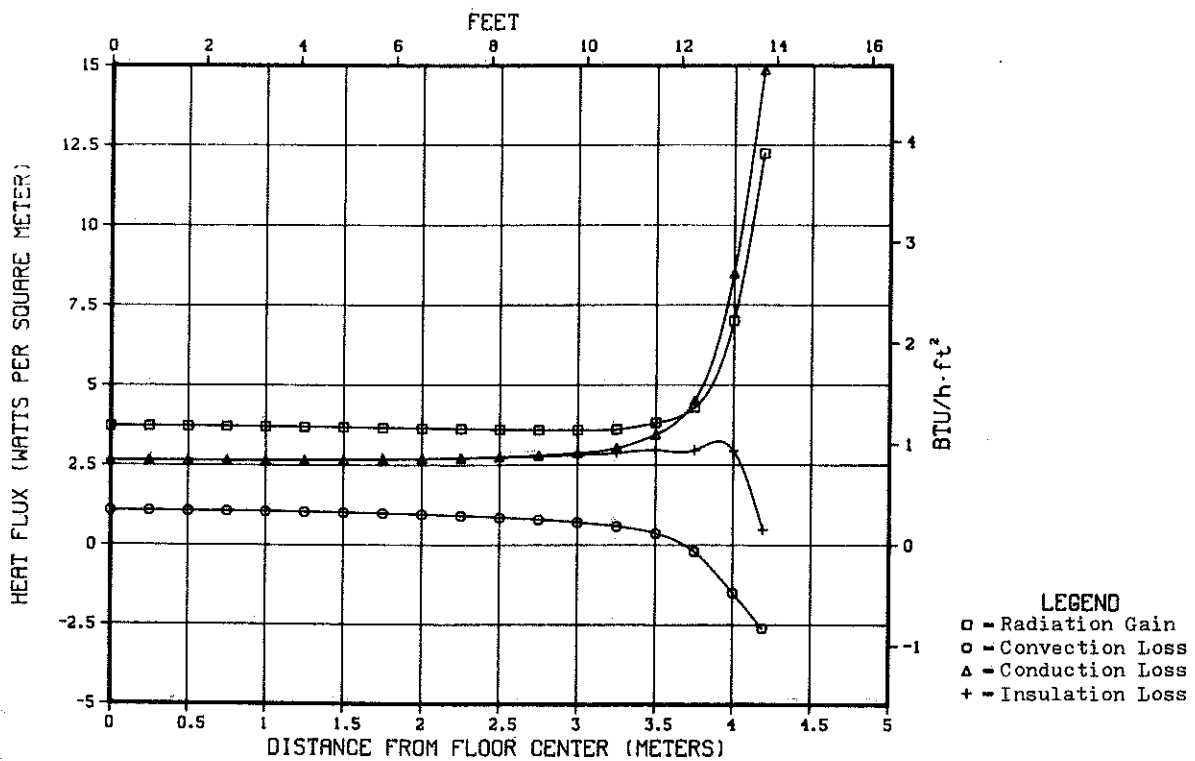


Figure 6. Heat flux profiles for House 2 at and below basement floor surface. Transient finite element model simulation, January 6, 1984

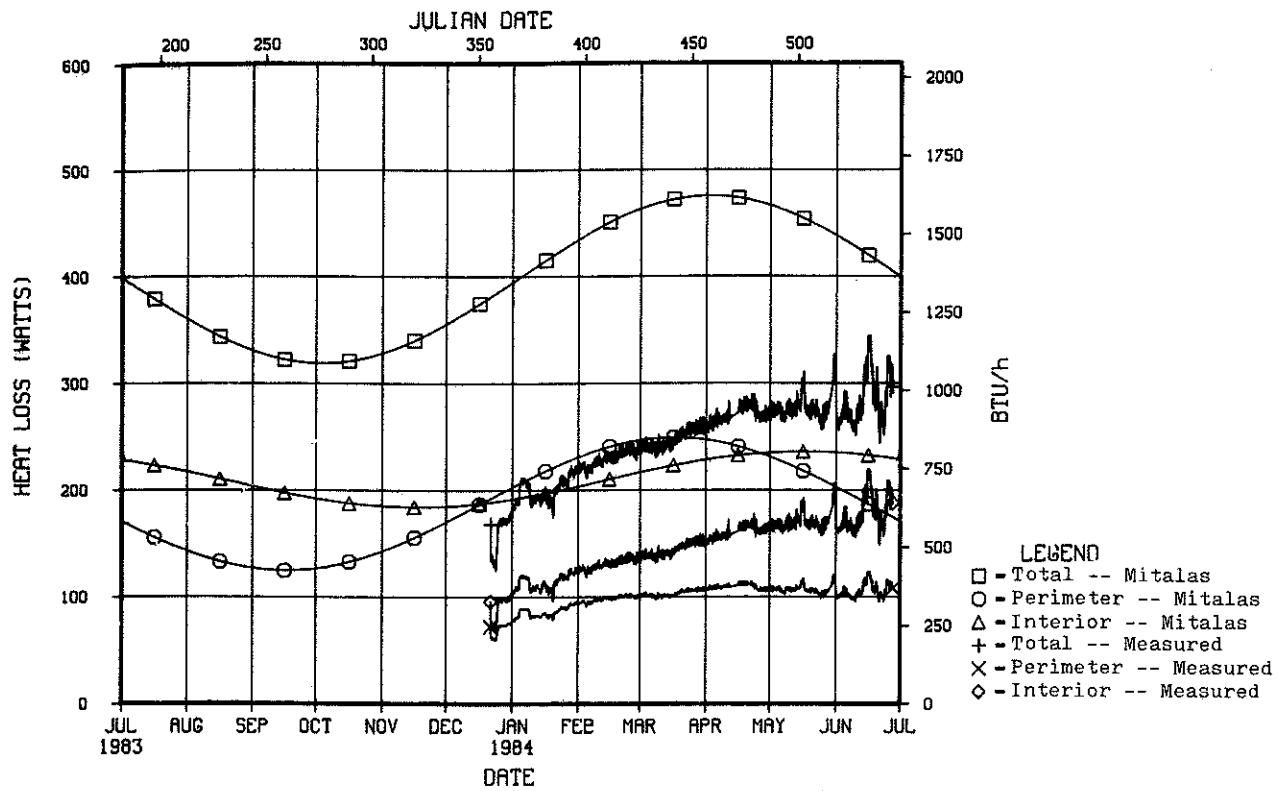


Figure 7. Comparison of measured basement floor heat losses for House 1 and those predicted with Mitalas' model

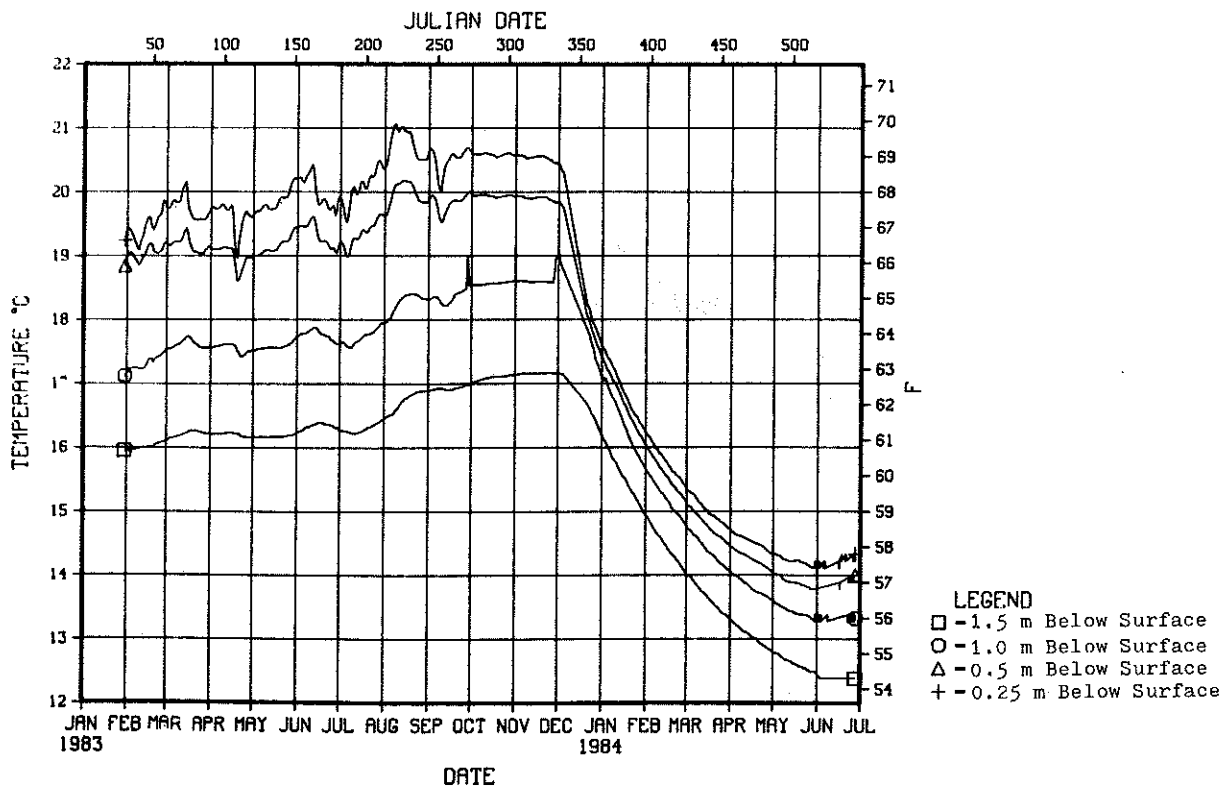


Figure 8. Measured ground temperatures beneath basement floor of House 1 at site "N"

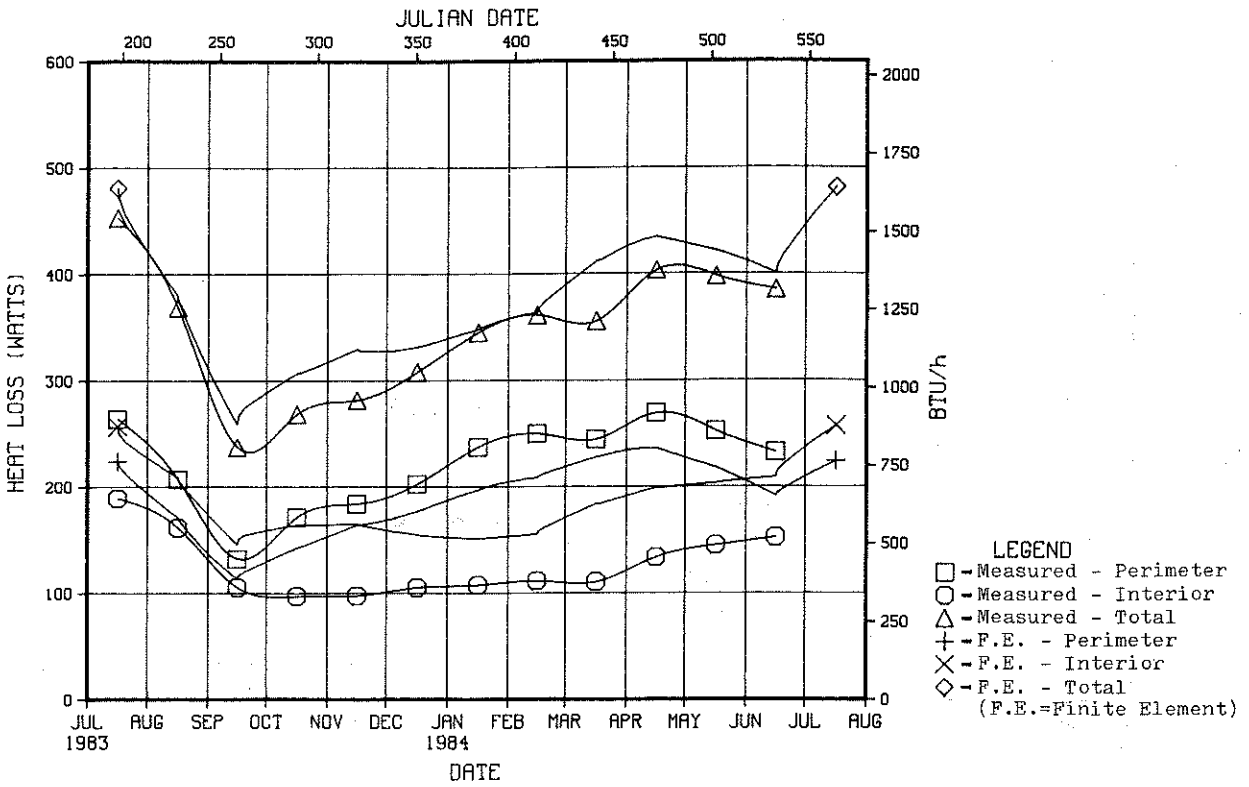


Figure 9. Comparison of measured basement floor heat losses for House 2 and those predicted with a transient finite element simulation

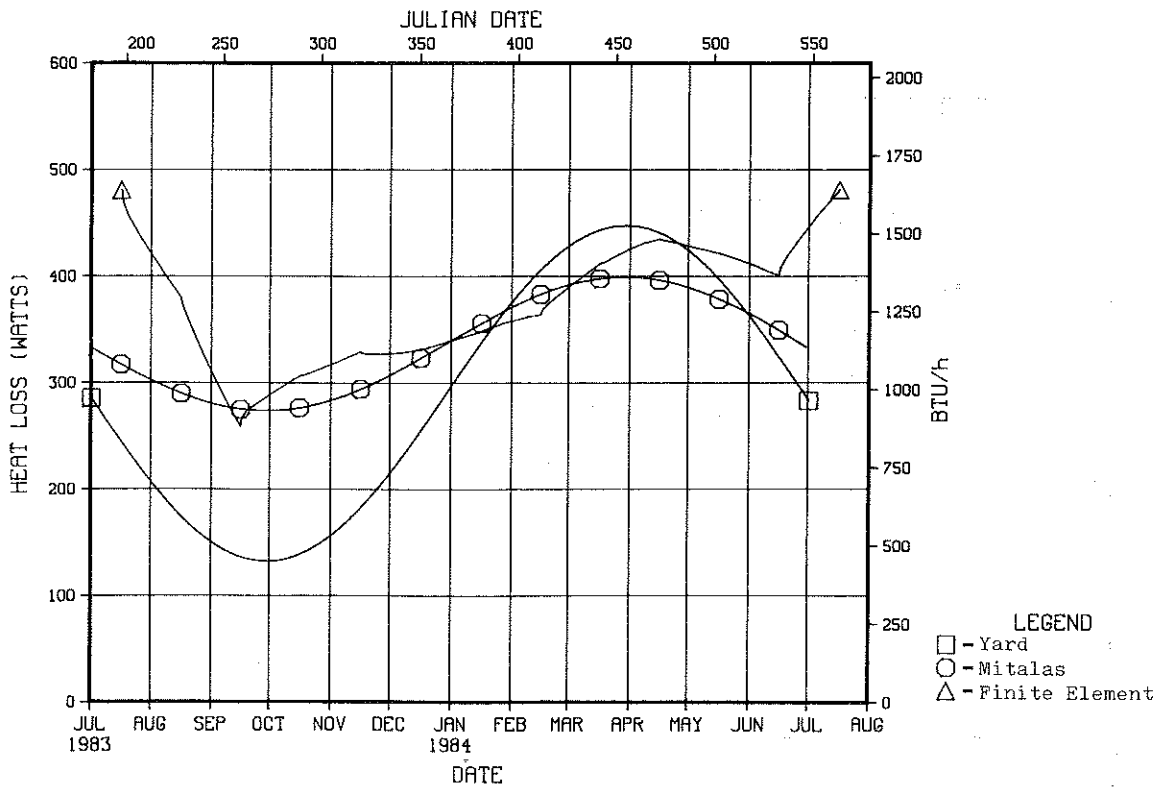


Figure 10. Comparison of basement floor heat losses predicted by Yard's model, Mitalas' model, and transient finite element simulation for House 2